Available online at www.sciencedirect.com
SCIENCE DIRECT®
ELSEVIER
Applied Surface Science 211 (2003) 236–243
applied surface science
www.elsevier.com/locate/apsusc

Metal–metal and metal–oxide interaction effects on thin film oxide formation: the Ti/TiO_2 and TiO_2/Ti cases

S.M. Mendoza*, L.I. Vergara, M.C.G. Passeggi Jr., J. Ferrón

INTEC, CONICET-Universidad Nacional del Litoral, Güemes 3450-CC91, 3000 Santa Fe, Argentina

Received 4 November 2002; received in revised form 13 February 2003; accepted 13 February 2003

Abstract

Through Auger electron spectroscopy (AES) and factor analysis (FA), we have studied the effect of metal–metal and metal–oxide interface interactions on the Ti oxide film formation. The passivation of Ti thin film oxidation is a thermally dependent process. It is possible, in consequence, to induce a further oxidation by heating the system. However, the complete oxidation of the thin film cannot be achieved in any case (for films thicker than 2 monolayers (ML)), due to substrate–Ti interactions. On the other hand, for the inverse configuration, metal over oxide, the strong Ti reactivity broadens the interface promoting the appearance of Ti_2O_3.

PACS: 82.80.Pv; 81.65.Mq

Keywords: Titanium oxides; Oxidation; Reduction; Thin film; AES; FA

1. Introduction

The applications of ultra-thin layers of metals deposited onto oxide surfaces and the formation of ultra-thin metal oxide films over metal or semiconductor surfaces are probably among the most widely used structures in basic physics and technology. In fact, their applications go from catalysis to microelectronic devices and from medicine to aircraft constructions. Since most of these metal–oxide and oxide–metal properties are determined by phenomena occurring at the interface, the understanding of the kinetic and thermodynamics features of the growth processes is a key point. The goal of this work is to understand the growth mechanisms and to learn about the realization of the desired structures.

Metal–metal oxide structures involving Ti are among the most interesting and used ones. Thus, the surface oxide passivation of Ti makes possible the biocompatibility of Ti and its use in medicine [1,2], and the production of protective coatings against corrosion [3]. On the other hand, metals over TiO_2 are widely used as catalyst, for instance in photolytic decomposition of water [4]. In a recent work, where we studied the transition of surface to bulk oxidation, we found that the oxidation regime in Ti thin films is strongly dependent on the film thickness [5]. We found that the oxidation process is characterized by the appearance of only TiO_2 for film thicknesses lower than 2 monolayers (ML) and a lower oxidation state of Ti (TiO_x with x close to 1) for intermediate film thicknesses. For thicker film as well as for bulk Ti,

* Corresponding author. Tel.: +54-342-4559174; fax: +54-342-4550944.
E-mail address: smendoza@intec.unl.edu.ar (S.M. Mendoza).

0169-4332/03/$ – see front matter
doi:10.1016/S0169-4332(03)00241-1

we detected only TiO_2. Recently we also showed that annealing in an oxygen atmosphere breaks the passivating effect enhancing the oxidation process. However, for the thinnest films studied (∼4 ML) the complete oxidation of Ti cannot be reached [6]. Related to the deposition of Ti on TiO_2, by means of XPS, Mayer et al. [7] observed that this process leads to an interfacial layer composed of reduced titanium oxides. They estimated that a deposition of 4 Å of Ti produces an interface layer of ∼12 Å thick.

In this work we present results, based on Auger electron spectroscopy (AES) and factor analysis (FA) [8], about the interface oxi-reduction reaction for the Ti/TiO_2 system. We study the controlled oxidation of Ti, prepared as a thin metallic film over a metallic substrate, and the subsequent chemical reaction of this oxide film when it is covered by a metallic Ti film.

2. Experimental setup and data treatment

2.1. Experimental setup

Measurements were performed in a commercial ultra-high vacuum (UHV) surface analysis system. The base pressure was in the 10^{-10} Torr range. Differentiated Auger spectra of the transitions Cu_{MNN}, Ti_{LMM}, Ti_{LMV} and O_{KLL} were acquired using a single-pass cylindrical mirror analyzer with a resolution of 0.6% and 4 V modulation amplitude. The primary electron beam energy was 3 keV, and the current density was 4 mA/cm^2. The electron gun was turned on only during the acquisition of the Auger spectra.

Titanium thin films were prepared by thermal evaporation from a high purity polycrystalline Ti bar that was heated through electron bombardment. Evaporation conditions could be accurately repeated by measuring the Ti bar temperature with a K-type thermocouple. Carbon and oxygen levels were carefully controlled with AES along the whole film growing process. Films were deposited on top of a Cu(1 0 0) monocrystal, which was cleaned by cycles of Ar^+ ion bombardment (1 keV) followed by annealing at 850 K until carbon and oxygen contamination was below the AES detection limit. During Ti evaporations, the Cu substrate was at room temperature (RT). UHV conditions were kept throughout the evaporations with chamber pressures in the 10^{-10} Torr range. The evaporation rate was checked before and after each experiment, and a typical value was 0.25 ML/min.

Ti oxidation was performed with high purity oxygen (better than 99.997%) that filled the whole UHV chamber, but it was evacuated during the AES acquisitions. The pressure was measured by means of a non-corrected Bayard–Alpert gauge.

A backside filament heated the sample radiatively, and the temperature was measured by means of a K-type thermocouple, attached to the edge of the sample.

2.2. Data treatment

The method of factor analysis [8] has been successfully applied on different analysis techniques including AES [9–13], and it is currently included as a standard data treatment system in most data treatment packages. The application of PCA in the sequential way to study chemical reactions occurring at surfaces and during depth profiling of reactive interfaces, has been extensively discussed in previous works [5,11,12,14]. Therefore, we will limit here ourselves to a brief description of the method.

In PCA, one works with the covariance matrix ($\boldsymbol{A}$) formed with the data matrix ($\boldsymbol{D}$); $\boldsymbol{A} = \boldsymbol{D}^{\boldsymbol{T}} \times \boldsymbol{D}$. In any sequential process involving AES, like an oxidation study, $\boldsymbol{D}$ is a $m \times n$ matrix whose n columns are formed by the Auger spectra acquired sequentially during the experiment, being each spectrum formed by m (energy) channels. The rank of $\boldsymbol{A}$ will be equal to the number of independent components of $\boldsymbol{D}$. Therefore, for a set of perfectly noise-free spectra, the determination of the number of independent chemical components is reduced to the determination of the number of non-zero eigenvalues of $\boldsymbol{A}$. Since noise is always present in a real experimental case, all eigenvalues of $\boldsymbol{A}$ are different from zero. Thus, the key point in PCA is the determination of those eigenvalues that have physical meaning, i.e. those eigenvalues which are statistically different from zero [11].

The last step in this method is the decomposition of the data matrix in a product of two matrices, in such a way that one matrix contains the Auger spectra of the pure components and the other one their relative weights [8,11]. This step, the so-called target transformation (TT) method, requires additional information. In the conventional TT one needs to know the concentration of $c - 1$ components in at least one

point of the profile. On the other hand, in the sequential method, the number of eigenvalues is fixed and the evolution of the error performed in reproducing the data matrix is followed as a new spectrum, following the sequence of the experiment, is added [11]. Each time the error in reproducing the data matrix with N fixed independent factors turns to be larger than the experimental error, it is necessary to assume the existence of a new factor in the process, i.e. from this point on, the system must be characterized by the presence of $N + 1$ components.

3. Results and discussion

In this work we performed different types of experiments involving metallic Ti and Ti oxides thin films. In a first step we analyzed the growth of a Ti thin film over a Cu(1 0 0) substrate. The second stage involves the Ti film oxidation, which is carried out in two steps: oxidation at room temperature up to saturation (including an overexposure), and post-oxidation. The post-oxidation process consists in heating the sample (600 K) keeping the oxygen in the chamber until a new saturation state is obtained. Finally, the third step corresponds to the growth of Ti over the oxidized film.

In Fig. 1 we show the peak-to-peak intensities corresponding to the Cu_{MNN} (60 eV), Ti_{LMV} (418 eV), and O_{KLL} (509 eV) Auger transitions as a function of the Ti evaporation time during thin film growth. The O_{KLL} intensity is plotted to show the low level of contamination achieved along the whole film growth process. The breaks observed in the time evolution of both Cu and Ti peaks correspond to the completion of successive layers [5]. The lines are least-square fits to the experimental data. This result shows a layer-by-layer growth of Ti over Cu(1 0 0), in agreement with previous findings [15]. Curves like the one shown in Fig. 1 are used along this work as a calibration curve to determine Ti film thickness. To control changes in the evaporation rate, calibration curves are repeated periodically. This procedure is really important when Ti films are grown over a Ti oxide substrate where the knowledge of the evaporation rate is the only way to determine the actual Ti coverage. This fact is accomplished calibrating the evaporator before and after each run. A Ti evaporation rate of around 0.25 ML/min is obtained from the figure for this particular calibration condition.

In Fig. 2 we show the evolution of the Auger line shape corresponding to the Ti_{LMM}, Ti_{LMV} and O_{KLL} transitions for the three different experiments performed along this work. The Cu_{MNN} Auger transition is not shown. In Fig. 2a we show the evolution of the Auger line shape along the growth of a Ti thin film over the Cu(1 0 0) substrate. At low coverages, the

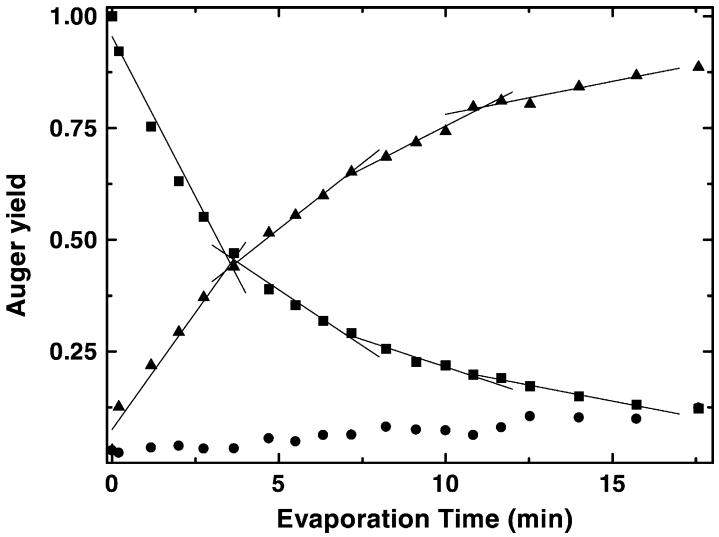

Fig. 1. Evolution of the Cu_{MNN} (■),Ti_{LMV} (▲), and O_{KLL} (●) peak-to-peak Auger yields (normalized to clean Cu signal) as a function of Ti evaporation time. The breaks in the curve represent the completion of each layer.

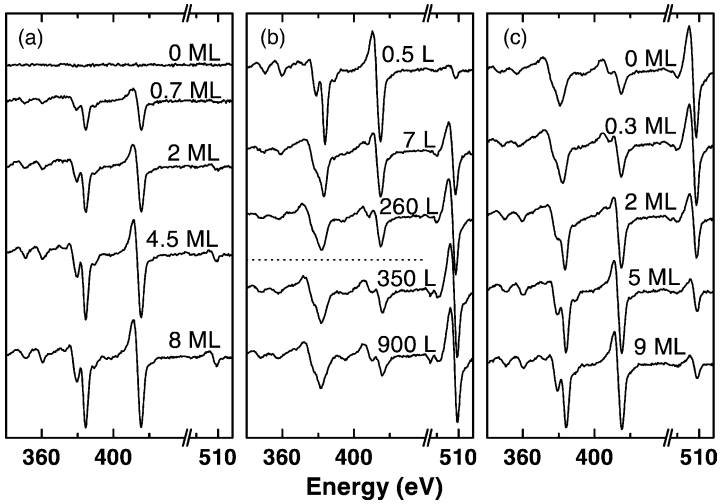

Fig. 2. Ti_{LMM} (340–400 eV), Ti_{LMV} (400–440 eV), and O_{KLL} (490–520 eV) Auger line shape evolution for: (a) growth of a Ti film over the Cu substrate; (b) Ti thin film oxidation and post-oxidation (below the dashed line); and (c) growth of a Ti film over TiO_2.

Ti_{LMV} signal shows a partial electron transference from Ti to Cu as we have already pointed out [5]. For thicker films, the typical Auger line shape of Ti transitions is recovered. In Fig. 2b, the evolution of the Auger line shapes during the oxidation of the thin film obtained in the first part of the experiment is depicted. The typical oxidation features are clearly observed; the fast growing of the O_{KLL} signal is accompanied by the evolution of the Ti Auger transition showing the depletion of the metallic valence band and the appearance of the inter atomic Ti–O transition at around 407 eV [16]. Below the dashed line we display the post-oxidation step. Heating the sample produces a further oxidation until a new saturation stage is reached. Finally, in Fig. 2c we show the evolution of the Auger line shape for the Ti deposition over the oxidized substrate. Roughly, the amount of Ti deposited over the Cu substrate is the same as in the first experiment (Fig. 2a). The strong interaction of Ti with the oxidized surface is qualitatively evident from the simple observation of the line shape evolution. In Fig. 3 we study these results in a more quantitative way by analyzing the evolution of the O_{KLL} and Ti_{LMV} Auger yields (peak-to-peak heights in the derivative spectra) (Fig. 3a, c and e), and the ratio between Ti_{LMV} and Ti_{LMM} Auger yields, hereinafter R_{VM} (Fig. 3b, d and f). Since only in Ti_{LMV} Auger transition Ti valence electrons are involved, the R_{VM} ratio is currently used as a rough indicator of the Ti oxidation state [14,16,17].

The results corresponding to Ti evaporation over Cu (Fig. 3a and b) show a Cu–Ti interaction at the interface. This interaction is apparent from the evolution of the R_{VM} ratio for Ti coverages <2 ML (Fig. 3b). The initial value of R_{VM} ($\sim$1.0) points out an electron transfer from the Ti valence band to Cu. For coverages beyond 2 ML, the bulk Ti value for R_{VM} ratio is recovered.

In Fig. 3c we observe the two known evolution stages for the O_{KLL} yield, in the Ti oxidation process: the initial fast increase followed by the slowing down of the oxygen sticking and the plateau which denotes the saturation regime. Since we are interested in the growth of Ti over TiO_2, and we know that at RT the Ti passivation occurs before the complete reaction of the Ti film [6], we induced the oxidation beyond this saturation by heating in an oxygen atmosphere, the partially oxidized film [6]. Heating the sample enhances Ti reactivity and oxygen diffusion, so the oxidation process restarts after a slight oxygen depletion. A second saturation stage, characterized by a larger amount of oxygen at the surface and a lower R_{VM} ratio (Fig. 3d), is obtained. The R_{VM} value shows a stronger final oxidation state and indicates that the formed oxide is nearly TiO_2.

Finally, in Fig. 3e and f we show the evolution of O_{KLL} and Ti_{LMV} Auger yields and the R_{VM} ratio during the growth of Ti over a TiO_2 film. The R_{VM} ratio points out the evolution from TiO_2 to Ti, but it does not allow

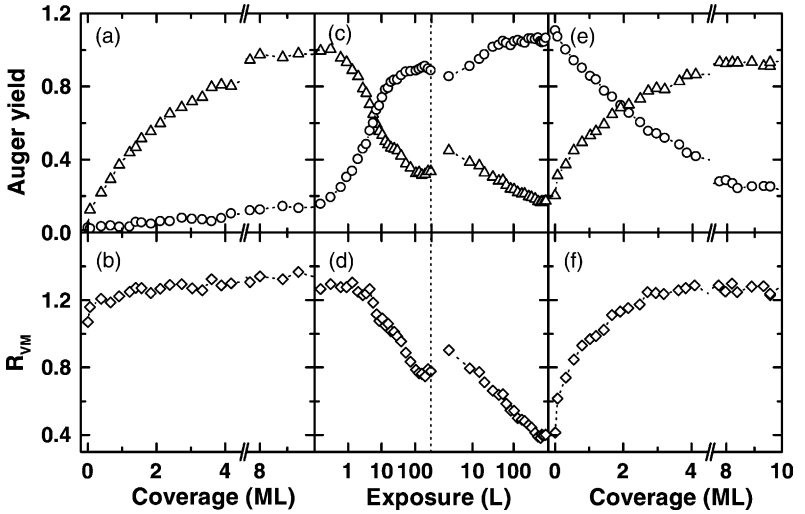

Fig. 3. Evolution of Ti_{LMV} (△) and O_{KLL} (○) peak-to-peak heights and R_{VM} ratio (◇) for: (a) and (b) growth of a Ti film over a Cu substrate; (c) and (d) Ti thin film oxidation and post-oxidation (beyond the dashed line); and (e) and (f) growth of a Ti film over TiO_2.

us to distinguish among a Ti–TiO_2 mixture and the presence of different sub-oxides. Comparing the growing rate of R_{VM} for the deposition of Ti over a metallic substrate (Fig. 3b) and over the oxidized substrate (Fig. 3f), for the same Ti coverage, we can observe the different reactivity of both interfaces.

To understand all the features involved in the Ti oxi-reduction process, we analyze the evolution of errors in FA as it was described in Section 2. In Fig. 4 we show the evolution, in the sequential analysis, of the error performed in reproducing the data matrix (***D***) by using one, two, and three factors for the evolution of the Ti Auger line shape during the Ti oxidation process and the growth of Ti over the oxidized film. Each time that in the sequential way the error overcomes the experimental error, a new factor

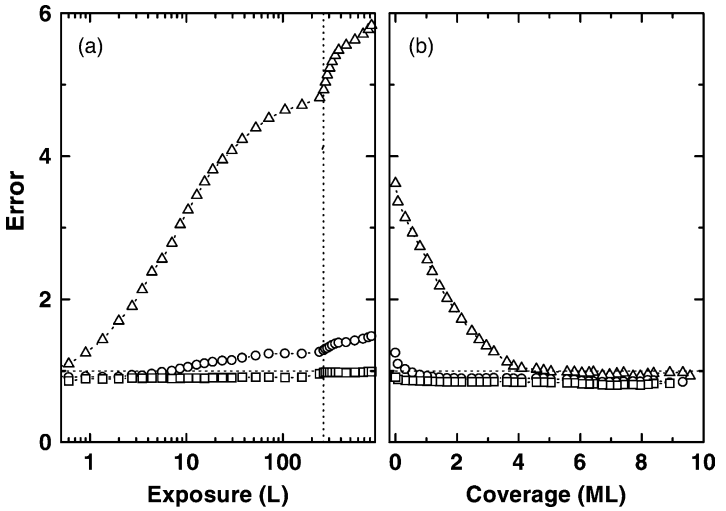

Fig. 4. Error evolution within the FA sequential analysis for: (a) Ti thin film oxidation and post-oxidation (beyond the dashed line) and (b) growth of a Ti film over TiO_2. Considering only one factor (△); adding a second factor (○); and including a third one (□).

(independent Auger spectrum) is needed to describe the evolution. Within this context, three factors are needed to reproduce the Auger data along the complete process for both experiments, i.e. oxidation and Ti growing over the oxide film. Note that the sequential analysis in the last case is reversely performed, i.e. we start from the final situation, where we can ensure the existence of only one factor, Ti^0. The fast reduction of the titanium oxide by the metallic Ti produces a fast disappearance of the corresponding factor, that is present at most in four Auger spectra, making the identification of this third factor less clear than in the oxidation process. Since the appearance of each factor is not simultaneous, the target transformation can be applied sequentially. Additionally, we know that the starting Auger spectrum in the oxidation process, and the ending one in the Ti growth, correspond to pure Ti. We also know that the oxidation of Ti thin films is characterized by the appearance of TiO_2 and TiO_x with x close to 1 [5]. This fact favors a rapid identification of Ti oxidized states. In Fig. 5 we show the Auger pure spectra obtained from TT analysis, compared with standard Auger line shapes for Ti [18] and its oxides; TiO [19], Ti_2O_3 [20] and TiO_2 [14]. We clearly identify the presence of Ti and TiO_2 as expected for both experiments, and the presence of TiO for the Ti thin film oxidation, and Ti_2O_3 for the metallic film growing over the oxidized one.

In Fig. 6 we show the evolution of the weights of each independent factor in the total Auger line shape for both experiments, along the complete processes. For a Ti thin film, the oxidation process at RT stops before the complete oxidation of the film, and the oxide film is a mixture of TiO_2 and TiO. The oxide film passivates the surface as in the bulk case [21], but the presence of the metallic substrate precludes the formation of a stoichiometric oxide. Heating the sample restarts the process breaking the passivation effect of the oxide film producing a further oxidation. A second saturation stage is reached, but as in the first stage, the film is not completely oxidized. For the range in which TiO appears (2 ML < thickness < bulk condition), we have found that the presence of this Ti sub-oxide depends on the presence of the metallic substrate and not on the Ti film thickness [6]. In fact, TiO is found for films thinner than Ti Auger electron escape depth, and for large exposures and high temperatures.

The growth of Ti over TiO_2 is characterized by a fast disappearance of TiO_2 (Fig. 6b) and the simultaneous appearance of Ti_2O_3 and Ti. This effect leads us to perform the sequential analysis in the reversal mode, where we can ensure only one factor as we noted previously. The appearance of Ti^{3+} clearly suggests the chemical reduction of Ti^{4+} due to Ti^0. Comparison of the actual Ti^{4+} evolution with respect to the

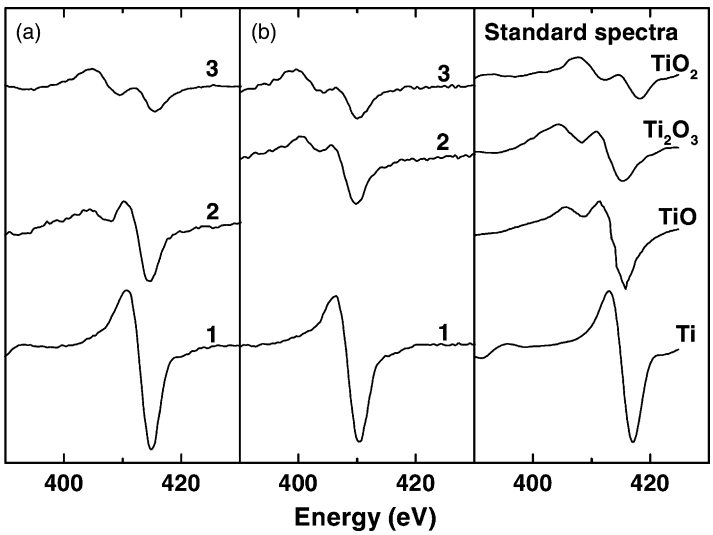

Fig. 5. Auger line shapes obtained from TT analysis for the same set of experiments displayed in Fig. 4: (a) Ti thin film oxidation and post-oxidation and (b) growth of a Ti film over TiO_2. Right panel: standard spectra for Ti and its different oxides.

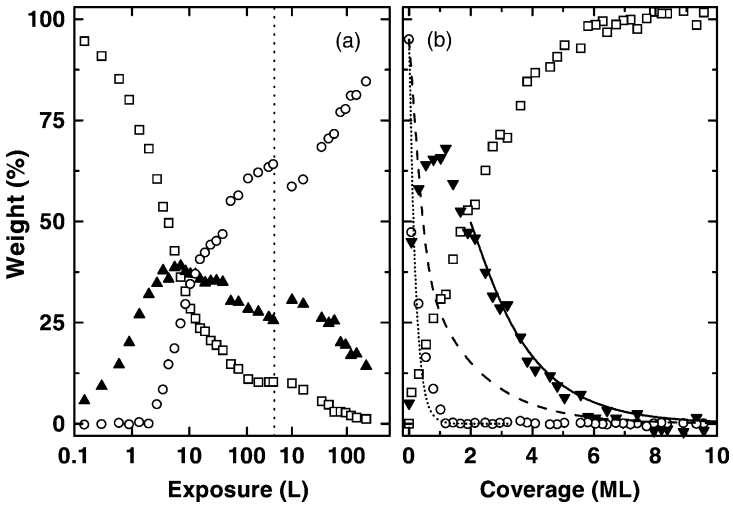

Fig. 6. Evolution of the weights of the different factors obtained through TT analysis for the same set of experiments shown in Fig. 4: (a) Ti thin film oxidation and post-oxidation (beyond the dashed line) and (b) growth of a Ti film over TiO_2. (- - -) Expected evolution of a pure non-reacted attenuation of Ti^{4+}. (···) Expected evolution of Ti^{4+} attenuation assuming that Ti_2O_3 is forming at the interface. (—) Expected evolution of a pure non-reacted attenuation of Ti^{3+}. (□) Ti, (▲) TiO, (▼) Ti_2O_3, and (○) TiO_2.

expected one for reacted and non-reacted interfaces strongly supports this idea. In fact, in Fig. 6b we display the Ti^{4+} weight evolutions calculated assuming the attenuation by a pure Ti film with an abrupt interface (dashed line in Fig. 6b) and by a reacted Ti/TiO_2 film (dotted line). In this last case we assume that each Ti monolayer produces three Ti_2O_3 layers [7]. In Fig. 6b we see a clear agreement between the experimental evolution and the expected one based on the reacted interface. On the other hand, the evolution of Ti^{3+} actually follows a pure attenuation depth evolution (solid line), suggesting a non-reacted Ti_2O_3/Ti interface. These results allow us to fully understand the growth of Ti over TiO_2. In fact, while Ti almost completely reacts with TiO_2 to form Ti_2O_3, the Ti/Ti_2O_3 interface is non-reactive. Thus, once the first Ti^0 monolayer has reacted with TiO_2 to form Ti_2O_3, creating a separation layer between the growing Ti and the subsurface TiO_2, the chemical reaction stops, no less Ti oxidized states (TiO_x with $x \leq 1$) appear, and the attenuation evolution follows a pure physical one. Our results are in close agreement with the work of Mayer et al. [7]. Based on XPS and LEIS measurements, they found the formation of an interfacial reduced layer and the reduced reactivity of the Ti/Ti_2O_3 interface compared with the Ti/TiO_2 one. On the other hand, while they suggest that the interface is a mixture of reduced oxide phases, from AES and FA we find that the interface is formed by Ti_2O_3.

Although thermodynamic concepts may be not valid in non-equilibrium reactions, in this case, the observed ones are just the reactions we would expect at room temperature based on those concepts. In this way, the reaction $Ti + 3TiO_2 \rightarrow 2Ti_2O_3$ ($\Delta G = -48$ kcal/mol) will be favored over the other possible one, $Ti + TiO_2 \rightarrow 2TiO$ ($\Delta G = -21.5$ kcal/mol) [22]. Finally, the other possible reaction, $Ti + Ti_2O_3 \rightarrow 3TiO$, appears as non-favored from thermodynamic arguments ($\Delta G = 0$) [22] in agreement with its absence along our experiments.

4. Conclusion

We have characterized, through Auger electron spectroscopy and factor analysis, the oxidation and reduction processes of Ti under different thin film regimes. We found that the passivating effects along oxidation and reduction processes have different origins: (i) the formation of TiO_2 prevents the subsequent Ti thin film oxidation, but the chemical reaction can be re-started, and the saturation regime changed by thermal activation. (ii) The presence of the metallic substrate inhibits, in any case, the complete thin film

oxidation, i.e. no matter the oxygen exposure or the substrate temperature, TiO is always present at the interface for films thicker than 2 ML. (iii) Ti_2O_3 stabilizes the interface ($TiO_2/Ti_2O_3/Ti$) precluding a further oxide reduction. The metal–metal and oxide–metal interactions preclude the obtention of either sharp metal–oxide or oxide–metal interfaces.

Acknowledgements

This work has been financially supported through PID 4799 from CONICET, CAI + D 2000 from UNL, PICT 03-04172 from the ANPCyT and 13783/1-22 from Fundación Antorchas. We wish to thank Dr. R. Vidal for his suggestions.

References

[1] U. Muller, R. Hauert, Thin Solid Films 290–292 (1996) 323.
[2] T. Hanawa, M. Ota, Appl. Surf. Sci. 55 (1992) 263.
[3] J.P. Espinós, A. Fernández, A.R. González, Surf. Sci. 295 (1993) 402.
[4] A.L. Linsebigler, G. Lu, J.T. Yates, J. Chem. Rev. 95 (1995) 735.
[5] I. Vaquila, M.C.G. Passeggi Jr., J. Ferrón, Phys. Rev. B 55 (1997) 13925.
[6] L.I. Vergara, M.C.G. Passeggi Jr., J. Ferrón, Appl. Surf. Sci. 187 (2002) 199.
[7] J.T. Mayer, U. Diebold, T.E. Madey, E. Garfunkel, J. Electr. Spectrosc. Rel. Phenom. 73 (1995) 1.
[8] E. Malinowski, D. Howery, Factor Analysis in Chemistry, Wiley, New York, 1980.
[9] V. Atzrodt, H. Lange, Phys. Status Solidi A 79 (1983) 489.
[10] V. Atzrodt, H. Lange, Phys. Status Solidi A 79 (1984) 373.
[11] R. Vidal, J. Ferrón, Appl. Surf. Sci. 31 (1988) 263.
[12] L. Steren, R. Vidal, J. Ferrón, Appl. Surf. Sci. 29 (1987) 418.
[13] J. Steffen, S. Hofmann, Surf. Sci. 202 (1988) L607.
[14] I. Vaquila, M.C.G. Passeggi Jr., J. Ferrón, Surf. Sci. 292 (1993) L795.
[15] C. Argile, G.E. Rhead, Surf. Sci. Rep. 10 (1989) 277.
[16] E. Roman, S.-M. Avedillo, J.L. de Segovia, Appl. Phys. A 35 (1984) 40.
[17] C.N. Rao, D.D. Sarma, M.S. Hedge, Proc. R. Soc. London A 370 (1980) 269.
[18] L.E. Davis, N.C. Mac Donald, P.W. Palmberg, G.E. Riach, R.E. Weber, Handbook of Auger Electron Spectroscopy, Perkin-Elmer, Eden Prairie, 1978.
[19] J.S. Solomon, W.L. Baun, Surf. Sci. 51 (1975) 228.
[20] V.M. Bermudez, J. Vac. Sci. Technol. 20 (1982) 51.
[21] I. Vaquila, M.C.G. Passeggi Jr., J. Ferrón, Appl. Surf. Sci. 93 (1996) 247.
[22] Handbook of Chemistry and Physics, 69th ed., CRC Press, Boca Raton, 1988.